Delay Aware Resource Management for Grid Energy Savings in Green Cellular Base stations with Hybrid Power Supplies

Vinay Chamola, Biplab Sikdar and Bhaskar Krishnamachari

***Abstract*—Base stations (BSs) equipped with resources to harvest renewable energy are not only environment-friendly but can also reduce the grid energy consumed, thus bringing cost savings for the cellular network operators. Intelligent management of the harvested energy can further increase the cost savings. Such management of energy savings has to be carefully coupled with managing the quality of service so as to ensure customer satisfaction. In such a process, there is a trade-off between the energy drawn from grid and the quality of service. Unlike prior studies which mainly focus on network energy minimization, this paper proposes a framework for jointly managing the grid energy savings and the quality of service (in terms of the network latency) which is achieved by downlink power control and user association reconfiguration. We use a real BS deployment scenario from London, UK to show the performance of our proposed framework and compare it against existing benchmarks. We show that the proposed framework can lead to around 60% grid energy savings as well as better network latency performance than the traditionally used scheme.**

***Index Terms*—Green communications, resource management, solar energy, base stations, cellular networks.**

I. Introduction

To cater to the increasing cellular traffic demands, there have been increasing number of cellular BSs deployments by telecom operators across the globe. This has not only increased the operational expenditure of the operators, but has also led to an increase in the contribution of cellular networks to the global carbon emissions. This has led to a number of initiatives from not only telecom operators but also government agencies and researchers to bring down the power consumption in these networks. Base stations contribute to around 60% of the power consumption in cellular networks. Thus powering base stations by renewable energy is one of the promising solutions for addressing this problem and such a solution has been already adopted by many telecom operators across the world [1]. According to a survery by Global System Mobile Association (GSMA) these deployments grew from just 9000 in the year 2010 to 43,000 in year 2014, showing 5 fold increase in a span of 4 years [2].

Locations that are very rich in solar resources can have base stations completely powered by solar energy. However, for locations with occasional bad weather periods, the size of harvesters and storage devices (e.g. PV (photo-voltaic) panels and batteries) required becomes very large which leads to very high CAPEX (capital expenditure), thus discouraging operators from adopting such a solution [3]. In such scenarios and in scenarios where the BSs are already connected to the grid, using renewable energy in conjunction with grid energy is a more viable approach. Powering the BSs by solar energy can reduce the grid energy consumption. Intelligent management of the harvested solar energy by such BSs and cooperation among them can lead to further reduction in the grid energy consumption in the network. Note that while doing so, the operators also have to take into account the quality of service (QoS) offered to the users in terms of the network latency, and have to consider the trade-off between cost savings and the network latency. Existing literature on joint management of grid energy consumption and the network latency uses only user-association reconfiguration to achieve the same. Additionally, some works propose dynamic BS operation (i.e. BS on/off strategies) which is also a means of bringing about grid energy savings through network energy minimization. In contrast to these approaches, we propose the use of intelligent green energy allocation and the use of down-link power control and user-association reconfiguration to address the problem. The efficacy of the proposed methodology has been shown by simulations using real BS deployment and solar energy traces for London, UK and by comparison against existing benchmarks. The major contributions of this paper can be summarized as follows:

- We consider a network of BSs powered by grid and solar energy, and formulate the problem of managing the grid energy savings and its trade-off with the network latency. We define a trade-off factor which captures the contribution of the grid energy consumed and the system latency in the objective function.
- Unlike existing literature which has used only user-association reconfiguration as a means to manage the grid energy savings while accounting for the network delay performance, we use BS downlink transmit power control in addition to user-association reconfiguration and show its performance gains. As the problem of downlink

Manuscript received Apr. 14, 2016; revised Aug. 10, 2016 and Oct. 9, 2016; accepted Oct. 21, 2016. Date of publication XX XX, 2016; date of current version XX XX, 2016. The associate editor coordinating the review of this paper and approving it for publication was K. Tourki. This work was supported by the Ministry of Education, Singapore under grant R263-000-A81-133.

Vinay Chamola and Biplab Sikdar are with the Department of Electrical and Computer Engineering, National University of Singapore, Singapore 11907 (e-mail:vinay.chamola.nus@gmail.com, bsikdar@nus.edu.sg).

B. Krishnamachri is with the Department of Electrical Engineering, University of Southern California, Los Angeles, CA 90089, USA (e-mail: bkrishna@usc.edu).

Digital Object Identifier: 10.1109/TCOMM.2016.2629502

power control is non-convex with respect to the problem of managing the grid energy savings and network delay, we propose a greedy heuristic algorithm to achieve the power control operations. We also provide an optimal user-association policy which minimizes the objective function value given the BSs operating at power levels decided by the power control algorithm.
- Majority of existing literature dealing with green cellular networks considers a time snapshot problem where the consumption of resources is minimized for an instant of time. However, such schemes do not address the problem of green energy allocation over time. In this paper, we propose a simple algorithm which guides the temporal allocation of green energy over time so as to maximize the benefit derived from it.
- We provide numerical results showing the trade-off between the grid energy consumption and the network latency for the proposed scheme. We also show the superiority of the proposed scheme over existing state-of-the-art benchmarks.

The rest of this paper is organized as follows. Section II presents a brief overview of related works. Section III describes the system considered in the paper. Section IV presents the problem formulation. Section V presents the solution methodology. Section VI presents the numerical results and Section VII concludes the paper.

II. Related Work

One of the possible ways of bringing grid energy savings in a network of grid-connected solar-powered BSs is to reduce the energy consumption in the network. In related work, authors in [4] propose dynamic BS switching to minimize the network energy consumption. The energy savings in dynamic BS switching is brought by switching off some of the BSs during low traffic periods. The authors in [5] present a practical scheme (named SWES) for the implementation of dynamic BS switching for a network of BSs. The scheme is a greedy heuristic which seeks to determine the minimum number of BSs to be switched on in order to serve the given area with a desired quality of coverage. BS switching for renewable energy powered cellular networks is considered in [6]. The problem of grid energy minimization is formulated and the BS on/off strategy to solve the problem is derived through a two-stage dynamic programming algorithm. In [7] the authors consider the problem of resource allocation and admission control in an OFDMA network and propose an algorithm for dynamic power adaptation of femtocells to minimize the overall power consumption of the network. An energy-efficient scheme for resource allocation in OFDMA systems with hybrid energy harvesting BSs is proposed in [8]. The scheme uses a stochastic dynamic programming approach for power allocation to minimize the network energy consumption. The authors in [9] propose an algorithm for green energy aware load balancing. The approach is based on tuning the beacon power levels (and not the actual transmit power levels) of the various BSs. By doing so, users are discouraged from joining BSs running low on green energy. In [10], the authors propose a Lyapunov optimization approach for bringing grid energy savings in a network of BSs where some of the BSs are connected to the grid whereas some are not. Note that all of the above studies primarily focus on minimizing the overall network energy consumption and most of them neglect the effect of doing so on the delay experienced by the users in the network. Some of the recent studies addressing network delay include [11] which proposes a distributed user association scheme using primal-dual formulation for traffic load balancing. The authors of [12] propose an α-optimal user association for the flow level cell load balancing with the objective of maximising the throughput or minimizing the system delay. However the above-mentioned schemes ([11],[12]) do not account for the green energy availability at the BSs.

Methodologies which consider the green energy availability in addition to the delay performance of the system include [13], [14], [15] and [16]. These studies address the issue of bringing grid energy savings while managing the quality of service (in terms of the network latency) [17]. The authors in [13]-[14] propose the GALA scheme which accounts for the green energy availability at the BS while making user-association decisions. The authors formulate the problem of minimizing the sum of weighted latency ratios of the BSs where the weights are chosen to account for the green energy availability at the BSs. The authors of [15] consider BSs powered by hybrid supplies and formulate the problem of minimizing the weighted sum of the cost of average system latency and the cost of on-grid power consumption. The authors of [16] also consider BSs powered by hybrid supplies but formulates the problem of lexicographic minimization of the on-grid energy consumption so as to reduce both total and peak on-grid energy consumption. The framework proposed in [16] introduces a penalty function to account for the network latency. The approach in [13], [15] and [16] to manage the available energy and network latency is by reconfiguring the BS-MT (mobile terminal) user-association. In contrast to such an approach, this paper presents a methodology for energy and latency management based on BS downlink transmit power control in addition to user association reconfiguration, and demonstrates its performance gains over existing approaches. The use of intelligent temporal energy allocation has been shown to have a superior performance in terms of managing the green energy and delay for an *off-grid scenario* in our previous work [18] [19]. In this paper we use insights from [18] and propose a temporal energy allocation scheme for *grid-connected* solar powered BSs. The works in [18], [19] focus on an off-grid scenario where the BSs are solely powered by solar energy, and consider the problem of minimizing the network latency. However this paper considers the scenario where the BSs not only harvest solar energy but can also draw energy from the grid. Thus BSs may draw energy from the grid to improve the network latency. The work in [18], [19] have only one parameter (i.e. the network latency) to be optimized. In contrast, the scenario of this paper requires both network latency and grid energy drawn to be optimized, which makes the problem more challenging.

III. System Model

In this section we describe the traffic model considered in the paper. We also describe the formulation of the BS load and the network latency.

A. Traffic Model, BS Load and Network Latency

Let us consider a region $\mathcal{X}$ served by a set, $\mathcal{B}$, of BSs. We use $x \in \mathcal{X}$ to denote the user location. For simplicity we primarily focus only on downlink communication (i.e. BSs to mobile terminals (MTs)). We denote the downlink transmit power levels of the BSs by a vector $\boldsymbol{P}$ where the transmit power levels can take discrete values i.e. $\boldsymbol{P}(j) \in \{0, \xi, 2\xi, \cdots, P_{max}\}$, where j is the index of the BS, ξ is the granularity of power control and P_{max} is the maximum transmit power level allowed. File transfer requests are assumed to arrive following a Poisson point process with an arrival rate $\lambda(x)$ per unit area at location x, with average file size of $\tau(x)$ bytes. We define the traffic load density at location x as $\gamma(x) = \lambda(x)\tau(x)$, where $\gamma(x)$ captures the spatial traffic variability. The rate offered at location x served by a BS j can be generally given using the Shannon-Heartley theorem [12] as

$$r_j(x) = BW_j \log_2(1 + SINR_j(x)) \tag{1}$$

where BW_j is the total bandwidth offered by the j-th BS and $SINR_j(x)$ is given by

$$SINR_j(x) = \frac{g_j(x)\boldsymbol{P}(j)}{\sigma^2 + \sum_{k \in I_j} g_k(x)\boldsymbol{P}(k)} \tag{2}$$

where $g_j(x)$ denotes the channel gain between the j-th BS and the user at location x which accounts for the path loss and the shadowing loss, σ^2 denotes the noise power level and I_j is the set of interfering BSs for BS j. This paper assumes perfect information of the channel gain which may be estimated given the topological details of the terrain, and drive-through site surveys. We introduce a user association indicator function $q_j(x)$ which indicates if the user at location x is served by BS j. If that is true then this variable has the value 1, and 0 otherwise. The BS load ρ_j, which denotes the fraction of time the BS j is busy serving its traffic requests can thus be given as [13]

$$\rho_j = \int_{\mathcal{X}} \frac{\gamma(x)}{r_j(x)} q_j(x) dx. \tag{3}$$

Definition 1: We denote the feasible set of the BS loads $\boldsymbol{\rho} = (\rho_1, \cdots, \rho_{|\mathcal{B}|})$ by $\mathcal{F}$ which can be defined as

$$\mathcal{F} = \Big\{ \boldsymbol{\rho} \mid \rho_j = \int_{\mathcal{X}} \frac{\gamma(x)}{r_j(x)} q_j(x) dx, \ 0 \le \rho_j \le \rho_{th}, \ \forall j \in \mathcal{B}, \\ q_j(x) \in \{0,1\}, \sum_{j \in \mathcal{B}} q_j(x) = 1, \ \forall j \in \mathcal{B}, \ \forall x \in \mathcal{X} \Big\},$$

where ρ_{th} is a threshold on the permitted BS load to avoid congestion at a given BS.

Note that as traffic requests follow a Poisson processes, the sum of such requests at a given BS is also a Poisson process. Further, as the BS's service time follows a general distribution, its operation can be modeled as a M/G/1 processor sharing queue. The average number of flows at BS j can thus be given by $\frac{\rho_j}{1-\rho_j}$ [15]. According to Little's law, the delay experienced by a traffic flow is directly proportional to the average number of flows in the system [20]. Thus we take the total sum of the flows in the network as the network latency indicator, $\mathcal{D}$, which is given by [15]

$$\mathcal{D} = \sum_{j \in \mathcal{B}} \frac{\rho_j}{1 - \rho_j}. \tag{4}$$

Note that this indicator has been widely used in existing literature (e.g. in [5], [12], [13], [21]) to quantify the network latency performance.

B. BS power consumption

The base station power consumption consists of a fixed part and a traffic dependant part. This paper considers macro BSs where the power consumption for BS j, denoted by $\boldsymbol{L}(j)$, can be modeled as [22]

$$L(j) = P_0 + \Delta \boldsymbol{P}(j)\rho_j, \ \ 0 \le \rho_j \le 1, 0 \le \boldsymbol{P}(j) \le P_{max} \tag{5}$$

where P_0 is the power consumption at no load (zero traffic) and Δ is the slope of the load dependent power consumption.

C. Solar Energy Resource and Batteries

We consider solar irradiation data provided by National Renewable Energy Laboratory (NREL) for London, UK [23]. This data is fed to NREL's System Advisor Model (SAM), to obtain the hourly energy generated by a PV panel of a given rating. We assume that the BSs use lead acid batteries to store the excess energy harvested by the PV panels. These are a popular choice in storage applications on account of their lower cost and being more time tested than other alternatives.

IV. Problem formulation

This section describes the problem formulation. We begin by describing the mechanism for green energy allocation over time. This mechanism is an important pre-requisite before formulating the optimization problem which jointly manages the grid energy savings and the quality of service. After describing the green energy allocation scheme, we formulate the optimization problem.

A. Green Energy Allocation

The green energy available to the BSs is in the form of energy stored in the batteries and the energy harvested during the day. This budget of green energy available to a BS needs to be intelligently allocated during the different hours of the day so as to optimize the use of the green energy, and in turn to minimize the grid energy usage. The green energy allocation for a given hour is done based on the energy available in the BS's battery at that time and the energy expected to be harvested in future hours during the day. Additionally, to avoid battery degradation, we dis-allow the battery from discharging below a certain state of charge, νB_{cap} where B_{cap} denotes the battery capacity and ν is a value which decides the lower limit below which batteries are dis-allowed to discharge. The green

energy budget $\boldsymbol{\mathcal{M}}_t$ at the beginning of a hour t is the green energy available for allocation from that hour to the last hour of the day (i.e. $t = 24$). Please note that we use the subscript t to denote the value of the variable during the t-th hour throughout this paper. Considering the t-th hour of operation for the j-th BS, the green energy budget at the beginning of hour t, which is the overall green energy that can be used over a period begining from time t to the last hour of the day, can be given as

$$\boldsymbol{\mathcal{M}}_t(j) = \boldsymbol{B}_{t-1}(j) - \boldsymbol{B}_{cr}(j) + \sum_{h=t}^{24} \boldsymbol{\mathcal{H}}_h(j) \tag{6}$$

where $\boldsymbol{B}_{t-1}$ denotes the battery level at the end of the previous hour, and $\sum_{h=t}^{24} \boldsymbol{\mathcal{H}}_h(j)$ denotes the green energy to be harvested during the given hour and the coming hours of the day. The battery levels are dis-allowed to go below state of charge νB_{cap} at any point of time. Because the energy allocation is done based on the expected energy to be harvested during the day which is a random process, we add a margin of safety to reduce the likelihood that the battery level goes below νB_{cap}. Thus we take $B_{cr} = (1 + \beta)\nu B_{cap}$ where β is the safety margin. Based on the information of the energy budget available, we allocate green energy to the given hour in proportion to the traffic load in the given hour. Thus the green energy allocated by the BS j to the hour t is given by

$$\begin{aligned}\boldsymbol{G}_t(j) &= \boldsymbol{\mathcal{M}}_t(j)\frac{\boldsymbol{L}_t(j)}{\boldsymbol{L}_t(j) + \sum_{m=t+1}^{24} \boldsymbol{L}_m(j)} \\ &= \boldsymbol{\mathcal{M}}_t(j)\frac{P_0 + \Delta\boldsymbol{P}_t(j)\rho_j^t}{P_0 + \Delta\boldsymbol{P}_t(j)\rho_j^t + \sum_{m=t+1}^{24} \boldsymbol{L}_m(j)}\end{aligned} \tag{7}$$

where ρ_j^t denotes the load of BS j in the t-th hour. For sake of clarity we use the following notation

$$\boldsymbol{A}_t(j) = \Delta\boldsymbol{P}_t(j) \tag{8}$$

$$\boldsymbol{B}_t(j) = P_0 + \sum_{m=t+1}^{24} \boldsymbol{L}_m(j). \tag{9}$$

Thus the green energy allocated for the hour t is given by

$$\boldsymbol{G}_t(j) = \boldsymbol{\mathcal{M}}_t(j)\frac{\boldsymbol{A}_t(j)\rho_j^t + P_0}{\boldsymbol{A}_t(j)\rho_j^t + \boldsymbol{B}_t(j)}. \tag{10}$$

Note that the green energy allocated for a given hour cannot exceed the green energy available to the BS at that time. Thus we limit the value of $\boldsymbol{G}_t(j)$ to be always below $\boldsymbol{B}_{t-1}(j) - \nu\boldsymbol{B}_{cap}(j) + \boldsymbol{\mathcal{H}}_t(j)$ (i.e. the total green energy available for hour t.) The overall green energy allocated for hour t is therefore given by

$$\begin{aligned}\boldsymbol{G}_t(j) = \Lambda_t(j)\boldsymbol{\mathcal{M}}_t(j)\frac{\boldsymbol{A}_t(j)\rho_j^t + P_0}{\boldsymbol{A}_t(j)\rho_j^t + \boldsymbol{B}_t(j)} \\ +(1-\Lambda_t(j))\left(\boldsymbol{B}_{t-1}(j) - \nu\boldsymbol{B}_{cap}(j) + \boldsymbol{\mathcal{H}}_t(j)\right)\end{aligned} \tag{11}$$

where $\Lambda_t(j)$ is an indicator variable defined below. If $\boldsymbol{\mathcal{M}}_t(j)\frac{\boldsymbol{A}_t(j)\rho_j^t + P_0}{\boldsymbol{A}_t(j)\rho_j^t + \boldsymbol{B}_t(j)} < \boldsymbol{B}_{t-1}(j) - \nu\boldsymbol{B}_{cap}(j) + \boldsymbol{\mathcal{H}}_t(j)$, then the BS has sufficient energy to satisfy the proportional energy allocation in (10) and the variable $\Lambda_t(j)$ is set to 1, and to 0 otherwise. For ease of notation, we denote $(\boldsymbol{B}_{t-1}(j) - \nu\boldsymbol{B}_{cap}(j) + \boldsymbol{\mathcal{H}}_t(j))$ by G_{thresh}. Then, $\Lambda_t(j) = 1$ when

$$\begin{aligned}\boldsymbol{\mathcal{M}}_t(j)\frac{\boldsymbol{A}_t(j)\rho_j^t + P_0}{\boldsymbol{A}_t(j)\rho_j^t + \boldsymbol{B}_t(j)} < G_{thresh} \\ \Rightarrow\ \rho_j^t < \frac{\boldsymbol{B}_t(j)G_{thresh} - \boldsymbol{\mathcal{M}}_t(j)P_0}{\boldsymbol{\mathcal{M}}_t(j) - G_{thresh}}\end{aligned} \tag{12}$$

and if the above inequality is not satisfied, $\Lambda_t(j) = 0$.

The methodology for assigning the green energy described above has been summarized in Algorithm 1 as the load proportional energy allocation (LPEA) algorithm.

Algorithm 1 The LPEA Algorithm

```
for j = 1 : B do
    M_t(j) = B_{t-1}(j) − B_cr(j) + Σ_{h=t}^{24} H_h(j);
    if ρ_j^t < (B_t(j)G_thresh − M_t(j)P_0)/(M_t(j) − G_thresh) then
        Λ_t(j) = 1
    else
        Λ_t(j) = 0
    end if
    G_t(j) = Λ_t(j)M_t(j)(A_t(j)ρ_j^t + P_0)/(A_t(j)ρ_j^t + B_t(j))
    +(1 − Λ_t(j))(B_{t-1}(j) − νB_cap(j) + H_t(j))
end for
```

This paper assumes that all energy allocation operations are done by a central server. The central server is assumed to have perfect information of the renewable energy that is harvested during the day which can be implemented in real life using weather forecasts. In existing literature there are many methodologies which predict the solar energy generation (e.g. [24], [25]). Integrating them with weather forecasts can give a more accurate prediction. The proposed algorithm needs only an hourly estimate of the solar energy generation for the day (i.e. an estimate of solar energy generation for the whole day with time granulaity of one hour), making the task even simpler. Also, for the initial green energy allocation (using the LPEA algorithm), any arbitrary load profile (like the one in [3] or [26]) can be used. Note that this energy allocation is just an initialization step and the green energy allocation is later iteratively updated after the downlink power control operations as discussed in Section V-B.

The green energy allocated to the BS in a given hour, G_t, is used to power the BS. If it not sufficient, then additional energy is drawn from the grid. Thus the grid energy consumed by the network during hour t, denoted by $\mathcal{E}_t$, is given by

$$\mathcal{E}_t = \sum_{j\in\mathcal{B}} \max\left(0, \boldsymbol{L}_t(j) - \boldsymbol{G}_t(j)\right). \tag{13}$$

Lemma 1: *Grid energy is drawn by BS j in the t-th hour only if its load value is greater than a certain value given as follows*

$$\rho_j^t > \begin{cases} \frac{\boldsymbol{\mathcal{M}}_t(j) - \boldsymbol{B}_t(j)}{\boldsymbol{A}_t(j)} & \Lambda_t(j) = 1 \\ \frac{\boldsymbol{B}_{t-1}(j) - \nu\boldsymbol{B}_{cap}(j) + \boldsymbol{\mathcal{H}}_t(j) - P_0}{\boldsymbol{A}_t(j)} & \Lambda_t(j) = 0. \end{cases} \tag{14}$$

Proof. Considering BS j, the grid energy drawn by the BS can be written as

$$\mathcal{E}_t(j) = \max\left(0, \boldsymbol{L}_t(j) - \boldsymbol{G}_t(j)\right). \tag{15}$$

For energy to be drawn from the grid we need

$$\boldsymbol{L}_t(j) - \boldsymbol{G}_t(j) > 0. \tag{16}$$

Note that for clarity, we omit the subscript t in the later part of the proof. First we consider the case when the BS has sufficient green energy for the load proportional allocation in (10) (i.e. $\Lambda(j) = 1$). From (5) and (11), substituting the values of $\boldsymbol{L}$, $\boldsymbol{G}$ and $\Lambda(j)$ in 16 we have

$$\begin{aligned} & P_0 + \Delta\boldsymbol{P}(j)\rho_j - \boldsymbol{\mathcal{M}}(j)\frac{\boldsymbol{A}(j)\rho_j + P_0}{\boldsymbol{A}(j)\rho_j + \boldsymbol{B}(j)} > 0 \\ \Rightarrow \;& (\boldsymbol{A}(j)\rho_j + P_0)\left(1 - \frac{\boldsymbol{\mathcal{M}}(j)}{\boldsymbol{A}(j)\rho + \boldsymbol{B}(j)}\right) > 0. \end{aligned} \tag{17}$$

Note that as ρ_j, $\boldsymbol{A}(j)$ and P_0 are all positive, for the above inequality to be true we require the following

$$\begin{aligned} & 1 - \frac{\boldsymbol{\mathcal{M}}(j)}{\boldsymbol{A}(j)\rho_j + \boldsymbol{B}(j)} > 0 \\ \Rightarrow \;& \rho_j > \frac{\boldsymbol{\mathcal{M}}(j) - \boldsymbol{B}(j)}{\boldsymbol{A}(j)}. \end{aligned} \tag{18}$$

Next for the case when $\Lambda(j) = 0$, (16) can be written as

$$\begin{aligned} & P_0 + \Delta\boldsymbol{P}(j)\rho_j - (\boldsymbol{B}_{t-1}(j) - \nu\boldsymbol{B}_{cap}(j) + \boldsymbol{\mathcal{H}}_t(j)) > 0 \\ \Rightarrow \;& \rho_j > \frac{\boldsymbol{B}_{t-1}(j) - \nu\boldsymbol{B}_{cap}(j) + \boldsymbol{\mathcal{H}}_t(j) - P_0}{\boldsymbol{A}(j)}. \end{aligned} \tag{19}$$

This completes the proof of the lemma. ■

B. Problem Formulation

We consider the following problem of minimizing the grid energy drawn and its trade-off with the network latency which is formulated as problem [P1] and given by

$$\begin{aligned} \textbf{[P1]} \quad & \underset{\boldsymbol{P}_t,\ \boldsymbol{\rho}_t}{\text{minimize}} \quad \sum_{t=1}^{24} \left(\mathcal{D}_t(\boldsymbol{P}_t, \boldsymbol{\rho}_t) + \eta\mathcal{E}_t(\boldsymbol{P}_t, \boldsymbol{\rho}_t)\right) \\ & \text{subject to:} \quad \boldsymbol{\rho}_t \in \mathcal{F} \end{aligned}$$

where η is a parameter which controls the trade-off between grid energy savings and the delay performance. Note that for $\eta = 0$, the problem reduces to minimizing the network latency, whereas for $\eta \to \infty$ the problem becomes minimizing the grid energy consumed without considering the delay performance. We propose to solve the above problem by using BS downlink transmission power control and user-association reconfiguration which involves suitably tuning the BS transmit power levels ($\boldsymbol{P}_t$) and managing the BS loads ($\boldsymbol{\rho}_t$).

V. Solution Methodology

This section presents the proposed methodology for addressing the problem [P1]. We address the problem using BS downlink power control and user association reconfiguration. The proposed framework for addressing the problem is named Green energy and Delay aware - Renewable Asset and resource Management (GD-RAM).

The problem [P1] is very challenging on account of the complexity arising from the coupling between BS power levels and the resulting user-association. Thus to make our analysis tractable, we make the assumption of time scale separation between the user association process and the period over which the power level control decisions are made. The user association process happens at a much faster time-scale than the time scale at which the green energy availability and the network traffic load vary. Studies have shown that the green energy availability and traffic pattern is nearly constant during a given hour of the day [5]. Further, as the time scale for determining the power levels of the BSs is of the order of that of traffic pattern and green energy availability variation (i.e. hours), it is much greater than that of the user-association process. Hence, with this assumption we decompose our problem into two sub-problems, in which the BS power control problem is solved at a slower time scale than the user association problem. The BS power level decisions are made on an hourly scale whereas the user-association scheme is periodically updated on a faster time scale. These sub-problems are given as follows:

Algorithm 2 Sequence of operations

```
for t = 1 : 24 do
    while power control convergence do
        while user association convergence do
            Perform green energy allocation for given hour using the LPEA algorithm.
            Solve user association problem for the given hour using the allocated green energy and the predicted traffic.
        end while
        Solve power control problem for the underlying user-association determined in the inner loop.
    end while
end for
```

1) **User association problem:** For BSs operating with power levels specified by a vector P, the user association problem aims at load balancing (balancing the BS loads) so as to find the optimal BS load vector $\boldsymbol{\rho}$ that minimizes the objective function. This problem is denoted as [P-UA] and can be expressed as

$$\textbf{[P-UA]} \quad \underset{\boldsymbol{\rho}_t \in \mathcal{F}}{\text{minimize}} \quad \mathcal{D}_t(\boldsymbol{P}_t, \boldsymbol{\rho}_t) + \eta\mathcal{E}_t(\boldsymbol{P}_t, \boldsymbol{\rho}_t). \tag{20}$$

2) **BS power control problem:** The BSs try to adjust their power levels so as to minimize the objective function and the problem is denoted by [P-PC] which can be given as

$$\textbf{[P-PC]} \quad \underset{\boldsymbol{P}_t \subset \tilde{\boldsymbol{\mathcal{P}}}}{\text{minimize}} \quad \left\{\mathcal{Q}_t(\boldsymbol{P}_t) = \mathcal{D}_t(\boldsymbol{P}_t) + \eta\mathcal{E}_t(\boldsymbol{P}_t)\right\}. \tag{21}$$

where $\tilde{\boldsymbol{\mathcal{P}}}$ is the set of all possible power level vectors and $\mathcal{Q}_t(\boldsymbol{P}_t)$ is defined as the solution to the user association problem in (20). Next, Section V-A describes the solution methodology for addressing the user association problem whereas Section V-B describes the solution methodology for addressing the BS power control problem. Algorithm 2 summarizes the sequence of the various operations inovolved in solving the problem P1.

Remark: Note that problem P-UA does not have a sum-

mation over time because user-association is a continuous process where the set of active users changes with time. However the active users associate with the BSs according to the proposed user-association policy so as to minimize the objective function at a given time instant. Further the problem P-PC does not have summation because it is solved individually for every hour of the day, with user-association determined using the average traffic profile for that given hour.

A. Optimal User Association Policy

In this section we propose the user association policy which achieves the global optimal of value of the objective function (with BSs operating at a given set of power levels).

Since $q_j(x) \in \{0,1\}$, the set $\mathcal{F}$ is not convex. Thus, to formulate the problem [P-UA] as a convex optimization problem, we relax the constraint to $0 \leq q_j(x) \leq 1$. Here q_j can be interpreted as the probability that the user at location x associates with BS j. The relaxed set of BS loads, $\tilde{\mathcal{F}}$, can be given as

$$\tilde{\mathcal{F}} = \Big\{ \boldsymbol{\rho} \mid \rho_j = \int_{\mathcal{X}} \frac{\gamma(x)}{r_j(x)} q_j(x) dx, \ 0 \leq \rho_j \leq \rho_{th}, \ \forall j \in \mathcal{B}, \\ 0 \leq q_j(x) \leq 1, \sum_{j=1}^{|\mathcal{B}|} q_j(x) = 1, \ \forall j \in \mathcal{B}, \ \forall x \in \mathcal{X} \Big\}.$$

The feasible set $\tilde{\mathcal{F}}$ is convex. The convexity of $\tilde{\mathcal{F}}$ has been proved by the authors in [12]. The problem [P-UA] with the relaxation condition is denoted as [P-UAR] and can be given as

$$\textbf{[P-UAR]} \ \underset{\boldsymbol{\rho} \in \tilde{\mathcal{F}}}{\text{minimize}} \quad \mathcal{U}(\boldsymbol{\rho}) = \mathcal{D}(\boldsymbol{\rho}) + \eta \mathcal{E}(\boldsymbol{\rho}).$$

Remark: We drop the subscript t throughout this section as user association is an continuous process where the set of active users in the network keeps changing, but at all times they associate with the BSs according to the proposed user-association policy. Additionally, we drop P, as the time-scale of user-association problem is faster than that of the power control operations, and thus power levels of the BSs are assumed to be fixed during the user-association operations. Further for notational simplicity we denote the optimization function value in the problem [P-UAR] by $\mathcal{U}(\boldsymbol{\rho})$. Note that although we formulate the optimization problem [P-UAR] using $\tilde{\mathcal{F}}$, the user association algorithm which we propose in this paper determines the deterministic user association (belonging to $\mathcal{F}$). This is shown in Theorems 1 and 2.

The working of the proposed user association algorithm is described as follows. The proposed user association algorithm operates in an iterative way. The BSs periodically measure their traffic loads and use it to determine an operational variable (called coalition factors in this section) and advertise it to the MTs. The mobile terminals choose which BS to associate with based on these coalition factors in order to minimize the objective function. The association between the MTs and the BSs is updated until convergence. To ensure convergence of the scheme, we assume that the traffic arrival and departure processes occur at a faster time scale as compared to that at which the BSs broadcast their coalition factors. This ensures that the users are able to make their association decisions for the broadcasted coalition factors before the next broadcast of coalition factors by the BSs. We assume BSs to be synchronized, thus broadcasting their coalition factors at the same time. The proposed user-association scheme can be easily implemented in a distributed way where the BSs periodically broadcast their coalition factor that can be embedded in the the beacon signals of the BSs [32] and users can use them to choose which BSs to associate with as described above.

Next, we begin with describing the user side and the BS side algorithms for carrying out the proposed user association mechanism.

1) **User Side Algorithm:** We define the time between two successive BS-MT association updates as a time slot in our algorithm. At the start of k-th time slot, the BSs send their coalition factors to the users using a broadcast signal. The users at location x in turn choose the BSs they associate with based on the coalition factors. In this section, superscript k is used to denote the value of a particular variable at the beginning of the k-th time slot. The coalition factor broadcast by BS j is given as

$$\phi_j^k = \frac{\partial \mathcal{U}^k(\boldsymbol{\rho})}{\partial \rho_j^k} \\ = \frac{1}{(1-\rho_j^k)^2} + \eta \zeta_j \boldsymbol{A}(j) \left(1 - \Lambda(j) \boldsymbol{\mathcal{M}}(j) \frac{\boldsymbol{B}(j) - P_0}{(\boldsymbol{\mathcal{M}} \rho_j^k + \boldsymbol{B}(j))^2} \right) \tag{22}$$

where ζ_j is a variable which captures whether BS j is drawing power from the grid. If the BS is drawing power from the grid then this variable is 1, else it is set to zero. The MTs update their user association functions as

$$q_j^k(x) = \begin{cases} 1 & \text{if } j = \arg\max_{j \in \mathcal{B}} \frac{r_j(x)}{\phi_j^k} \\ 0 & \text{otherwise.} \end{cases} \tag{23}$$

Note that the association functions ($q_j(x)$) are indicator of which BS the MTs at location x associate with as discussed in Section III-A. The computational complexity of the user side algorithm for an individual user is $O(|\mathcal{B}|)$.

2) **BS side algorithm:** At the end of the k-th time slot, the BSs measure their load levels which we denote by $T_j(\rho_j^k)$, and is given as

$$T_j(\rho_j^k) = \min \left(\int_{\mathcal{X}} \frac{\gamma(x)}{r_j(x)} q_j(x) dx, \rho_{th} \right). \tag{24}$$

After measuring $T_j(\rho_j^k)$, the BS updates its traffic load which is used to evaluate the next coalition factor to be broadcast for time slot $k+1$ as [12]

$$\rho_j^{k+1} = \alpha \rho_j^k + (1-\alpha) T_j(\rho_j^k) \tag{25}$$

with $0 < \alpha < 1$ being an averaging exponential factor.

Next, the proof of convergence and optimality and convergence of the proposed user association algorithm is presented. We begin by showing that the objective function $\mathcal{U}$ is convex in $\rho \in \tilde{\mathcal{F}}$ in Lemma 2 which leads to Lemma 3 which shows that there is an unique optimal user association which minimizes

the objective function.

Lemma 2: *The objective function $\mathcal{U}(\boldsymbol{\rho}) = \mathcal{D}(\boldsymbol{\rho}) + \eta\mathcal{E}(\boldsymbol{\rho})$ is convex in $\boldsymbol{\rho}$ when $\boldsymbol{\rho}$ is defined on $\tilde{\mathcal{F}}$.*

Proof. This can be proven by showing that $\nabla^2\mathcal{U}_i(\boldsymbol{\rho}) > 0$. The objective function can be written in terms of $\boldsymbol{\rho}$ as

$$\begin{aligned}\mathcal{U}(\boldsymbol{\rho}) =\ & \mathcal{D}(\boldsymbol{\rho}) + \eta\mathcal{E}(\boldsymbol{\rho}) \\ =\ & \sum_{j\in\mathcal{B}}\left(\frac{\rho_j}{1-\rho_j} + \eta\zeta_j\left(L(j) - G(j)\right)\right) \\ =\ & \sum_{j\in\mathcal{B}}\left(\frac{\rho_j}{1-\rho_j}\right) \\ & + \sum_{j\in\mathcal{B}}\Bigg(\eta\zeta_j\Bigg(\boldsymbol{A}(j)\rho_j + P_0 - \Bigg(\Lambda(j)\boldsymbol{\mathcal{M}}(j)\frac{\boldsymbol{A}(j)\rho_j + P_0}{\boldsymbol{A}(j)\rho_j + \boldsymbol{B}(j)} \\ & + (1-\Lambda(j))\left(\boldsymbol{B}_{t-1}(j) - \nu\boldsymbol{B}_{cap}(j) + \boldsymbol{\mathcal{H}}_t(j)\right)\Bigg)\Bigg)\Bigg) \quad (26)\end{aligned}$$

We evaluate the first and second order derivatives of the objective function with respect to $\boldsymbol{\rho}$ which are given as

$$\begin{aligned}\nabla\mathcal{U}(\boldsymbol{\rho}) =\ & \sum_{j\in\mathcal{B}}\Bigg(\frac{1}{(1-\rho_j)^2} \\ & + \eta\zeta_j\boldsymbol{A}(j)\left((1-\Lambda(j))\boldsymbol{\mathcal{M}}(j)\frac{\boldsymbol{B}(j) - P_0}{(\boldsymbol{A}(j)\rho_j + \boldsymbol{B}(j))^2}\right)\Bigg) \quad (27)\end{aligned}$$

$$\begin{aligned}\nabla^2\mathcal{U}(\boldsymbol{\rho}) =\ & \sum_{j\in\mathcal{B}}\Bigg(\frac{2}{(1-\rho_j)^3} \\ & + 2\eta\zeta_j\boldsymbol{A}(j)^2\Lambda(j))\boldsymbol{\mathcal{M}}(j)\frac{\boldsymbol{B}(j) - P_0}{(\boldsymbol{A}(j)\rho_j + \boldsymbol{B}(j))^3}\Bigg). \quad (28)\end{aligned}$$

Note that all the addition terms in the function above are non-negative, and $\frac{2}{(1-\rho_j)^3}$ is always positive for all the BSs. Thus, the above term is always positive which proves that the function is convex. Also for the case when grid energy is not drawn, the component in the objective function for a particular BS just consists of the first term which is always positive. Thus even for the case when energy is not drawn from the grid, the objective function is convex in $\boldsymbol{\rho}$. ■

Remark: Note that as we consider the steady state analysis of the system, the proof above assumes that $\frac{\partial f(\rho_j)}{\partial \rho_g} = 0\ ,\ j \neq g$ ([9], [12], [15]) where $f(\rho_j)$ is purely a function of ρ_j and does not depend on ρ_g ($g \neq j$).

Lemma 3: *A unique optimal user association $\boldsymbol{\rho}^* \in \tilde{\mathcal{F}}$ exists which minimizes $\mathcal{U}(\boldsymbol{\rho}) = \mathcal{D}(\boldsymbol{\rho}) + \eta\mathcal{E}(\boldsymbol{\rho})$.*

Proof. It has been shown in Lemma 1 that the objective function $\mathcal{U}(\boldsymbol{\rho})$ is a convex function of $\boldsymbol{\rho} \in \tilde{\mathcal{F}}$. Thus there exists a unique optimal $\boldsymbol{\rho} = \boldsymbol{\rho}^*$ which minimizes $\mathcal{U}(\boldsymbol{\rho})$. ■

Next we prove the convergence of the proposed user-association algorithm. We begin with proving that $T_j(\boldsymbol{\rho}^k)$ gives a descent direction for $\mathcal{U}(\boldsymbol{\rho}^k)$ at $\boldsymbol{\rho}^k$ (shown in Lemma 4). Thus after some iterations the traffic load converges which is proved in Theorem 1. Further, in Theorem 2 we prove that the trafic load thus obtained minimizes the objective function $\mathcal{U}(\boldsymbol{\rho})$.

Lemma 4: *For $\boldsymbol{\rho}^k \neq \boldsymbol{\rho}^*$, $T_j(\boldsymbol{\rho}^k)$ gives a descent direction for $\mathcal{U}(\boldsymbol{\rho}^k)$ at $\boldsymbol{\rho}^k$.*

Proof. $\mathcal{U}(\boldsymbol{\rho})$ is a convex function of $\boldsymbol{\rho} \in \tilde{\mathcal{F}}$. Thus the fact that $T(\boldsymbol{\rho}^k)$ gives a descent direction to $\mathcal{U}(\boldsymbol{\rho}^k)$ at $\boldsymbol{\rho}^k$ can be easily proved by showing $< \nabla\mathcal{U}(\boldsymbol{\rho}^k), T(\boldsymbol{\rho}^k)) - \boldsymbol{\rho}^k > \leq 0$ (where $< a, b >$ denotes the inner product of vectors a and b) [33]. Let $q_j(x)$ and $q_j^T(x)$ be user association indicators which result in BS traffic ρ_j^k and $T(\rho_j^k)$, respectively. Then the inner product can be written as

$$\begin{aligned}& < \nabla\mathcal{U}(\boldsymbol{\rho}^k), T(\boldsymbol{\rho}^k) - \boldsymbol{\rho}^k > \\ & = \sum_{j\in\mathcal{B}}\left(\frac{1}{(1-\rho_j^k)^2} + \eta\zeta_j\boldsymbol{A}(j)\left(1 - \Lambda(j)\boldsymbol{\mathcal{M}}(j)\frac{\boldsymbol{B}(j) - P_0}{(\boldsymbol{A}(j)\rho_j^k + \boldsymbol{B}(j))^2}\right)\right) \\ & \qquad \times \left(T_j(\rho_j^k) - \rho_j^k\right) \\ & = \sum_{j\in\mathcal{B}}\left(\frac{1}{(1-\rho_j^k)^2} + \eta\zeta_j\boldsymbol{A}(j)\left(1 - \Lambda(j)\boldsymbol{\mathcal{M}}(j)\frac{\boldsymbol{B}(j) - P_0}{(\boldsymbol{A}(j)\rho_j^k + \boldsymbol{B}(j))^2}\right)\right) \\ & \qquad \times \left(\int_{\mathcal{X}}\frac{\gamma(x)(q_j^T(x) - q_j(x))}{r_j(x)}dx\right) \\ & = \int_{\mathcal{X}}\gamma(x)\sum_{j\in\mathcal{B}}\Bigg(\frac{\left(\frac{1}{(1-\rho_j^k)^2} + \eta\zeta_j\boldsymbol{A}(j)\left(1 - \Lambda(j)\boldsymbol{\mathcal{M}}(j)\frac{\boldsymbol{B}(j) - P_0}{(\boldsymbol{A}(j)\rho_j^k + \boldsymbol{B}(j))^2}\right)\right)}{r_j(x)} \\ & \qquad \times (q_j^T(x) - q_j(x))\Bigg)dx.\end{aligned}$$

Note that

$$\sum_{j\in\mathcal{B}}\frac{\left(\frac{1}{(1-\rho_j^k)^2} + \eta\zeta_j\boldsymbol{A}(j)\left(1 - \Lambda(j)\boldsymbol{\mathcal{M}}(j)\frac{\boldsymbol{B}(j) - P_0}{(\boldsymbol{A}(j)\rho_j^k + \boldsymbol{B}(j))^2}\right)\right)(q_j^T(x) - q_j(x))}{r_j(x)}$$

≤ 0 holds because q_j^T evaluated based on (23) maximizes the value of $\frac{r_j(x)}{\left(\frac{1}{(1-\rho_j^k)^2} + \eta\zeta_j\boldsymbol{A}(j)\left(1 - \Lambda(j)\boldsymbol{\mathcal{M}}(j)\frac{\boldsymbol{B}(j) - P_0}{(\boldsymbol{A}(j)\rho_j^k + \boldsymbol{B}(j))^2}\right)\right)}$. Thus we have $< \nabla\mathcal{U}(\boldsymbol{\rho}^k), T(\boldsymbol{\rho}^k) - \boldsymbol{\rho}^k > \leq 0$. ■

Theorem 1: *The traffic load $\boldsymbol{\rho}$ converges to the traffic load $\boldsymbol{\rho}^* \in \mathcal{F}$.*

Proof. We prove this by showing that $\boldsymbol{\rho}^{k+1} - \boldsymbol{\rho}^k$ is also a descent direction of $\mathcal{U}(\boldsymbol{\rho}^k)$. To show this we consider the following expression

$$\begin{aligned}\rho_j^{k+1} - \rho_j^k &= \alpha\rho_j^k + (1-\alpha)T_j(\rho_j^k) - \rho_j^k \\ &= (1-\alpha)(T(\rho_j^k) - \rho_j^k). \quad (29)\end{aligned}$$

In Lemma 3, it has been shown that $(T(\boldsymbol{\rho}^k) - \boldsymbol{\rho}^k)$ is a descent direction of $\mathcal{U}(\boldsymbol{\rho}^k)$. Further we have $(1-\alpha) > 0$ as $0 < \alpha < 1$, thus $\boldsymbol{\rho}^{k+1} - \boldsymbol{\rho}^k$ also gives the descent direction of $\mathcal{U}(\boldsymbol{\rho}^k)$. Additionally, as $\mathcal{U}(\boldsymbol{\rho}^k)$ is a convex function it can be easily concluded that $\mathcal{U}(\boldsymbol{\rho}^k)$ converges to $\boldsymbol{\rho}^*$. If $\mathcal{U}(\boldsymbol{\rho}^k)$ converges to any other point than $\mathcal{U}(\boldsymbol{\rho}^*)$, then $\boldsymbol{\rho}^{k+1}$ again gives a descent direction so as to decrease $\mathcal{U}(\boldsymbol{\rho}^k)$, which contradicts the assumption of convergence. Further, because $\boldsymbol{\rho}^k$ is derived based on (23) where $q_j(x) \in \{0, 1\}$, $\boldsymbol{\rho}^*$ is in the feasible set $\mathcal{F}$. ■

Theorem 2: *If the set $\mathcal{F}$ is non-empty and the traffic load $\boldsymbol{\rho}$ converges to $\boldsymbol{\rho}^*$, the user association corresponding to $\boldsymbol{\rho}^*$ minimizes $\mathcal{U}(\boldsymbol{\rho})$.*

Proof. Let $q^* = \{q_j^*(x) | q_j^*(x) \in \{0,1\}, \forall j \in \mathcal{B}, \forall x \in \mathcal{X}\}$ and $u = \{q_j(x) | q_j(x) \in \{0,1\}, \forall j \in \mathcal{B}, \forall x \in \mathcal{X}\}$ be the user association corresponding to $\boldsymbol{\rho}^*$ and $\boldsymbol{\rho}$, where $\boldsymbol{\rho}$ is some traffic load vector satisfying $\boldsymbol{\rho} \in \mathcal{F}$. As $\mathcal{U}(\boldsymbol{\rho})$ is a convex function over $\boldsymbol{\rho}$, the theorem can be proved by showing $< \nabla\mathcal{U}(\boldsymbol{\rho}^*), \Delta\boldsymbol{\rho} - \boldsymbol{\rho}^* > \geq 0$. In the proof below, we substitute $\frac{\partial\mathcal{U}(\boldsymbol{\rho}^*)}{\partial\rho_j^*}$ as $\phi_j(\rho_j^*)$ for notational clarity (these expressions are identical as shown in the derivation leading to (22). We have

$$\begin{aligned} < \nabla\mathcal{U}(\boldsymbol{\rho}^*), \boldsymbol{\rho} - \boldsymbol{\rho}^* > &= \sum_{j\in\mathcal{B}} \phi_j(\rho_j^*)\,(\boldsymbol{\rho} - \boldsymbol{\rho}^*) \\ &= \sum_{j\in\mathcal{B}} \left(\int_{\mathcal{X}} \frac{\gamma(x)(q_j(x) - q_j^*(x))}{r_j(x)\phi_j^{-1}(\rho_j^*)} dx \right) \\ &= \int_{\mathcal{X}} \gamma(x) \sum_{j\in\mathcal{B}} \frac{(q_j(x) - q_j^*(x))}{r_j(x)\phi_j^{-1}(\rho_j^*)} dx. \end{aligned}$$

But because the optimal user association is determined based on the following rule

$$q_j^*(x) = \begin{cases} 1, & \text{if } j = \arg\max_{j\in\mathcal{B}} \frac{r_j(x)}{\phi_j(\rho_j^*)}, \\ 0, & \text{otherwise.} \end{cases},$$

we can say that,

$$\sum_{j\in\mathcal{B}} \frac{q_j^*(x)}{r_j(x)\phi_j^{-1}(\rho_j^*)} \leq \sum_{j\in\mathcal{B}} \frac{q_j(x)}{r_j(x)\phi_j^{-1}(\rho_j^*)}. \tag{30}$$

Therefore, $< \nabla\mathcal{U}(\boldsymbol{\rho}^*), \boldsymbol{\rho} - \boldsymbol{\rho}^* > \geq 0$ which completes the proof. ■

B. Base Station Transmission Power Control

We assume that the power control operations are decided by the central server before a day begins and that guides the power levels of the BSs during the day. Further as the power level decisions are made on a time-scale of an hour, the power control operations just require the average traffic profile at a given location for each hour. We assume that the central server has this average traffic profile information which is used to evaluate the underlying user association for facilitating the power control decisions. There are a number of existing papers in literature which study, model and predict cellular network traffic like [27], [29] and [28] . The information/ideas from these models could be used in real time implementation of our work. Additionally, such information could be also predicted by the operators using the traffic pattern during past few weeks/months. Note that the above-mentioned assumptions have been considered in several contemporary works (e.g. [30], [31]). Next, we show an important observation about the downlink power control.

Proposition 1: *The objective function $\mathcal{Q}_t(\boldsymbol{P}_t) = \mathcal{D}_t(\boldsymbol{P}_t) + \eta\mathcal{E}_t(\boldsymbol{P}_t)$ is a non-convex function of the BS power levels.*

To verify this proposition using simulations, we consider a network of BSs as shown in Figure 2. The simulation settings are as described in Section VI. We consider BSs operating at 3 p.m ($t = 15$) on January 1st with BSs 2, 4, 5 and 6 operating at transmit power level 20 W. Next, we vary the power levels of BSs 1 and 3 and study the effect of the same on the objective

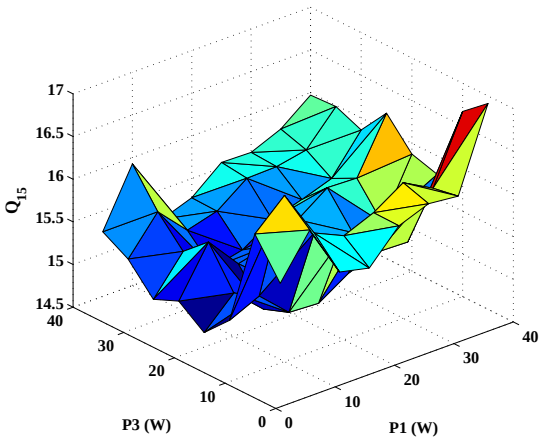

Fig. 1. Objective function ($\mathcal{Q}_t$) value variation with power control operations on BS 1 and BS 3 ($\eta = 2$, t =15).

function. Figure 1 shows the objective function (for $\eta = 2$) and from the figure we can easily conclude that the objective function is a non-convex function of the BS power levels.

As shown above, the power level control problem to minimize the objective function is a non-convex optimization problem. Finding the optimal solution for such a problem requires a search over the entire state space and has a very high computational complexity. The order of such computations increases exponentially with the number of BSs ($\mathcal{B}$) and the hours under consideration (denoted by T) and is given by $O(\mathcal{N}^{|\mathcal{B}|T})$ where $\mathcal{N}$ denotes the number of possible power levels the BSs can operate at. To make the power control approach feasible, we resort to developing a greedy heuristic for addressing the problem of power control and the proposed downlink transmit power control algorithm is presented in Algorithm 3.

The proposed algorithm is carried out sequentially for each hour of the day. The working of the downlink transmit power control algorithm can be explained as follows. For every hour, all the BSs start with a transmit power level of P_{max}. Next we check for which BS the decrement of power level brings the largest improvement in the objective function ($\mathcal{Q}_t$). The BS with the largest reduction in the objective function while satisfying the system constraints (which is tracked in the algorithm by the variable con) is chosen for transmit power reduction. This is done until no further improvement in the objective function can be realized. The improvement in the delay component of the objective function in the power control operations is due to its interference management and load balancing effect. The reduction in the grid energy consumption is due to the transmit power level of a BS low on green energy going down, and further, some users being offloaded (which reduces $\boldsymbol{\rho}$), thus decrementing the BS power consumption. The worst case computational complexity of this algorithm is $O(\mathcal{N}|\mathcal{B}|^2)$. Note that the load levels of the BSs change after every iteration of power control operations. Thus after this algorithm is carried out for all the hours of the day, we have different traffic load profiles for the different hours as

Algorithm 3 Downlink Transmit Power Control Algorithm

Initialization
Set $\boldsymbol{P}_t(j) = P_{max}$ for all $j \in \mathcal{B}$
Compute $\mathcal{Q}_t(\boldsymbol{P})$; Set $\delta\mathcal{Q} = 1$
while $\delta\mathcal{Q} > 0$ **do**
    $\mathcal{Q}_{old}$= $\mathcal{Q}_t(\boldsymbol{P}_t)$
    for $j = 1 : |\mathcal{B}|$ **do**
        $\boldsymbol{P}_{curr} = \boldsymbol{P}_t$
        $\boldsymbol{P}_{curr}(j) = \max(0, \boldsymbol{P}_t(j) - \xi)$
        $\mathcal{Q}'(j) = \mathcal{Q}_t(\boldsymbol{P}_{curr})$
        if $\max(\boldsymbol{\rho}) > \boldsymbol{\rho}_{th}$ **then**
            $con(j)$= 0
        else $con(j)$= 1
        end if
    end for
    a. z : index of BS having $con = 1$ for which power control leads to minimum objective function value ($\mathcal{Q}'$)
    b. Set $\mathcal{Q}_{new}$ = $\mathcal{Q}'(z)$
    $\delta\mathcal{Q} = \mathcal{Q}_{old} - \mathcal{Q}_{new}$
    if $\delta\mathcal{Q} > 0$ **then**
        $\boldsymbol{P}_t(z) = \max(0, \boldsymbol{P}_t(z) - \xi)$;
    end if
end while

compared to that used for initial energy allocation during the day (using Algorithm 1). Consequently, we repeat the energy allocation followed by another application of the downlink transmit power control algorithm for the day. After some iterations of doing this (typically 3-4 iterations) the solution for the downlink power levels converges. Note that the proposed power control approach does not guarantee an optimal solution but gives an local optimal solution. It follows the intution of greedy descent approach to minimize the objective function. At a given iteration, the BS for which the power level decrement leads to maximum delay reduction is chosen to be powered down. Thus the power levels for the next iteration gives a delay performance better than that at the previous iteration. Additionally as the number of power levels a BS can take are limited and lower-bounded by 0, the algorithm is guaranteed to converge.

VI. Numerical Results

For performance analysis of the proposed scheme, we consider a 3G BS deployment (shown in Figure 2) deployed by network provider Vodafone near Southwark, London, UK with 6 BSs providing coverage to an area of 1 km^2. The BSs are assumed to be equipped with PV panel with DC rating 6 kW and 10 batteries. We consider that the BSs use 12 V, 205 Ah flooded lead acid batteries. The carrier frequency is 2.5 GHz and we assume 10 MHz bandwidth with full frequency reuse. Log normal shadowing with standard deviation 8 dB with the correlation distance for shadowing taken as 50m has been considered [35]. We model the path loss, PL, as [34]

$$PL(dB) = 40(1 - 4 \times 10^{-3} h_{BS}) log_{10}(R) - 18 log_{10}(h_{BS}) + 21 log_{10}(f) + 80 \quad (31)$$

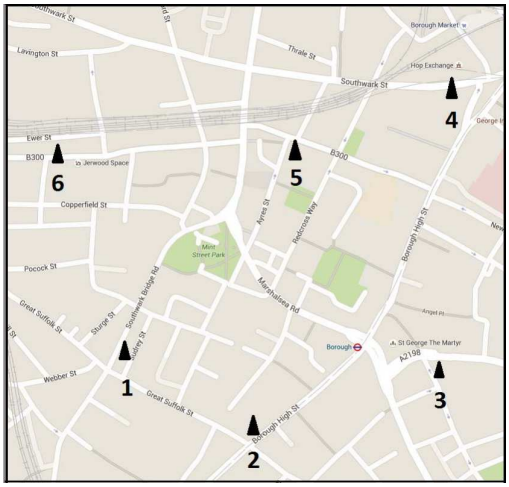

Fig. 2. 3G BS deployment near Southwark (London).

where R denotes the distance between the MT and the BS, h_{BS} is the base station antenna height above rooftop and f is the carrier frequency in MHz. We take h_{BS} as 15 meters and the carrier frequency is 2.5 GHz, based on the suggestions from the baseline test scenario mentioned in IEEE 802.16 evaluation methodology document [35]. Thus, the path loss is calculated as $PL(dB) = 130.19 + 37.6 \log(R)$. We take the noise power to be -174 dBm/Hz [35]. A homogeneous Poisson point process is used to generate the file transfer request. The rate of the Poisson process depends on the hour of the day, with the smallest number of file transfer requests during early morning hours (2-5 am) with an average of 20 requests per unit area (km^2) and the largest number of requests in the evening (5-7 pm) with an average of 200 requests per unit area. For weekends a lower traffic level with minimum and maximum number of file transfer requests (per unit area) of 10 and 150 respectively, in the corresponding hours have been considered. For simplicity, we assume that each file transfer request requires 50 KB of data traffic to be served. The entire area (of 1 km^2) is divided into 1600 locations with each location representing a 25 m x 25 m area. To model temporal traffic dynamics, a new spatial profile of file transfer requests is generated after every 2 minutes. The location based traffic load density is calculated based on the traffic model. For simulations we consider solar energy data obtained from NREL [23] for the month of January of typical meteorological year (TMY) data for London. Figure 3 shows the solar energy harvested by the PV panels during the different days of this month by the BSs (with PV panels having DC rating 6 kW). Additionally we assume that 1^{st} January is Monday (i.e. weekday load profile). The values of P_0, P_{max} and Δ used for the results were 412.4 W, 40 W and 22.6 respectively [22]. The granularity of the power control, ξ, was 5 W and $\boldsymbol{\rho}_{th}$ used for the results was 0.85. The value of ν, the limiting state of charge was taken as 0.3, and the safety margin β was taken as 0.1. The initial battery levels were randomly chosen for the different BSs for 1^{st} January. We take the averaging factor α for the BS side algorithm to be 0.95, and with this value the proposed user-association algorithm was observed to converge

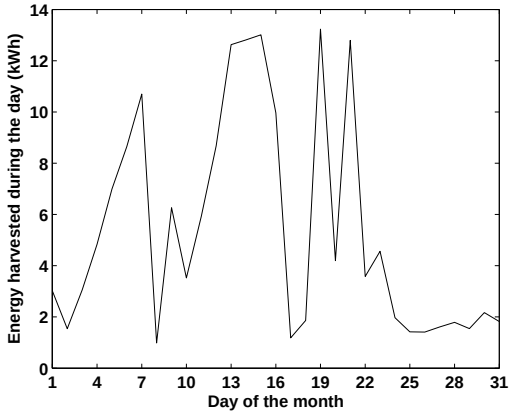

Fig. 3. Solar energy harvested during the day by the BSs for the month of January of Typical meterological year (TMY) for London (PV panel rating: 6 kW).

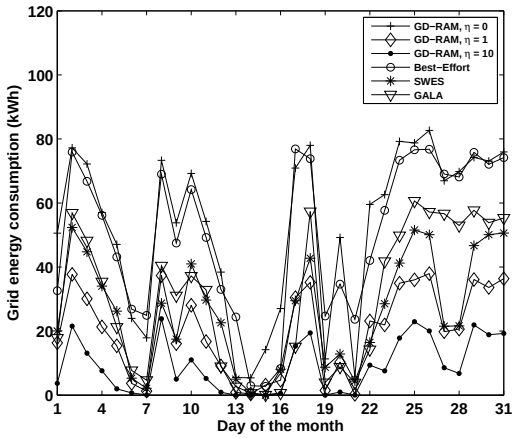

Fig. 4. Grid energy consumption for the different schemes.

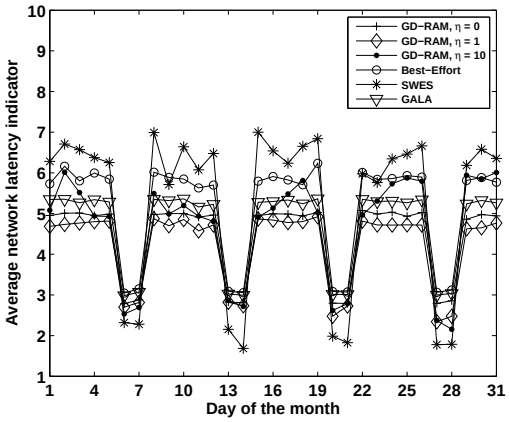

Fig. 5. Average network latency performance for the different schemes.

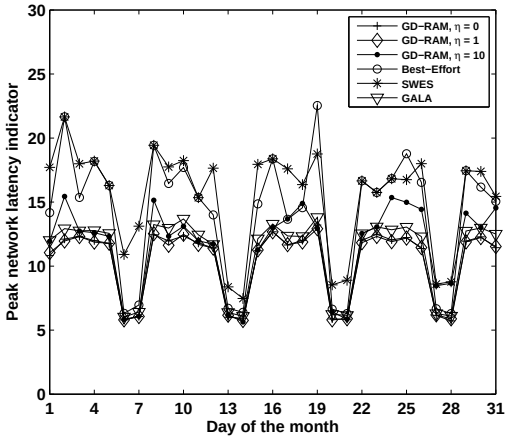

Fig. 6. Peak network latency performance for the different schemes.

to the optimal solution within 20 iterations.

As a benchmark for comparison, we consider a Best-Effort scheme where all BSs operate with transmit power 20 W and the MTs associate with the BS with the strongest signal strength at that location. BSs use green energy as long as it is available and after that draw energy form the grid. We also consider the GALA [13] scheme with BSs operating at transmit power 20 W, and the SWES [5] scheme which is a BS on-off scheme with BSs operating at 40 W when they are switched on. The GALA and the SWES scheme have been briefly described in Section II.

A. Grid Energy Savings

Figure 4 shows the grid energy consumption for the different schemes for the month of January. It can be seen that the Best-Effort scheme leads to very high values of grid energy consumption. The GALA scheme shows significant grid energy savings as compared to the Best-Effort scheme. Note that the SWES scheme has lower grid energy consumption than the Best-Effort and the GALA scheme. This is because in this scheme some of the BSs switch off to reduce the overall network power consumption. The BSs which are switched off save energy and the energy harvested during this period is stored in the batteries to be used for future hours, thus reducing the need to draw energy from the grid. The proposed GD-RAM scheme allows a wide range of control over the grid energy consumption. Note that with $\eta = 0$, the grid energy consumption is the highest which is comparable to the Best-Effort scheme. This is because for this case, the power control and user association operations are done solely considering the network delay. For $\eta = 1$, we observe that the grid energy consumed is smaller as compared to the other benchmark schemes. Further, for $\eta = 10$ the energy drawn from the grid is even smaller. Note that the grid energy savings in the SWES scheme and our scheme for $\eta = 10$ is at the expense of an increase in the network latency (Figure 5) which is discussed in the next subsection.

B. Delay Performance

Figures 5 and 6 show the average network latency and the peak network latency for the benchmark schemes and for the proposed scheme for three different values of the trade-off factor η for the days under consideration. Note that the

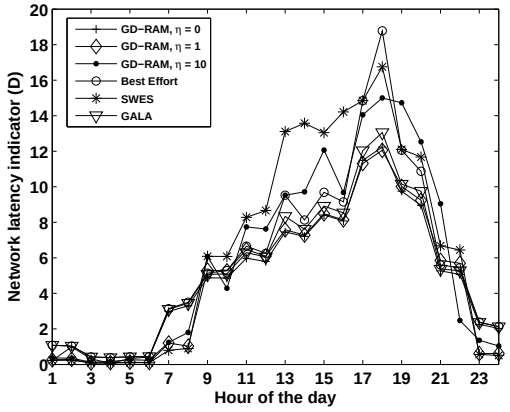

Fig. 7. Hourly network latency for the different schemes (25^{th} January).

proposed algorithm shows delay performance better than the Best-Effort and the SWES scheme for all three η values. The network latency performance of the GALA scheme is better than the Best-Effort and the SWES scheme. Note that for most of the days, the average latency for $\eta = 1$ is smaller than that for $\eta = 0$. This is because of the non-convexity of the objective function with respect to power control operations. Note that for $\eta = 1$, the BS power levels reduce to much lower values as compared to the case for $\eta = 0$, so as to bring grid energy savings. Our experiments show that at lower BS power levels, there is better interference management through the power control operations, thus also bringing down the network latency. However, for $\eta = 10$, on certain days which have very bad weather, the proposed scheme trades the network latency performance for bringing about grid energy savings. For example, the values of the average delay and peak delay on 25^{th} January (which is a bad weather day) for $\eta = 10$ are significantly higher than that for $\eta = 0$ and $\eta = 1$. However on good weather days, like 12^{th} January, the delay performance for $\eta = 10$ is comparable to that for $\eta = 0$ and $\eta = 1$. Additionally, the results show that the network latency is lower on weekends as compared to the weekdays. This is because the traffic to be served on these days is lower than that on weekdays. Note that the SWES scheme leads to a lower average delay on weekends as compared to all other schemes. This is because the traffic to be served during weekends is smaller and therefore most of the BSs turn off, thus reducing the interference to the BSs that are turned on. This contributes to reducing the system delay for the SWES scheme on these days. However on weekdays, as the traffic to be served is higher, turning off BSs has the effect of increasing the network latency as can be seen from the results. Figure 7 shows the hourly network latency for 25^{th} January. The network latency is low for all the schemes during the early morning hours due to the low traffic during those hours. However, during the daytime, the SWES scheme and the proposed scheme for $\eta = 10$ lead to a higher delay than the Best-Effort scheme. The GALA scheme and our proposed scheme (for $\eta = 0$ and $\eta = 1$) have better delay performance than the other benchmarks. Figure 8 shows the transmit power levels of the BSs on 25^{th} January for the GDRAM scheme for three different η values. Note that the power levels for $\eta = 0$ are relatively higher than for the cases when $\eta = 1, 10$. This is because for $\eta = 0$ the power control operations are aimed solely on delay reduction. As $\eta = 1$ also accounts even for the grid energy consumption, the power levels for this case are lower as compared to those with $\eta = 0$. For the case of $\eta = 10$, the power levels are still lower as compared to the case of $\eta = 1$.

C. Grid Energy Consumption and Delay Trade-off

Figures 9 and 10 show the grid energy consumption and delay trade-off for the proposed GD-RAM scheme for different trade-off parameter values and for the benchmark schemes (averaged for the month of January). Note that for GALA scheme, θ is the trade-off parameter and its value varies from 0 to 1. Figure 9 considers the trade-off between the grid energy consumption and the average (over 31 days) of the hourly network latency whereas Figure 10 considers the trade-off between the grid energy consumption and the average (over 31 days) of the daily peak network latency. We can observe that for the proposed scheme, as we start increasing η from 0, the average grid energy consumption reduces sharply while there is no degradation in the latency, rather there is a slight improvement in the network latency. The reason for this phenomenon is the non-convexity of the objective function with respect to power control operations. Note that as the η value increases from 0, the BS power levels become smaller in order to reduce the grid energy consumption. However, the power level adjustments are made while accounting for the network latency, in addition to accounting for the grid energy savings (as our objective function accounts for both). Figure 8 shows the transmit power levels for three different η values ($\eta = 0, 1$ and 10). For $\eta = 1$, the transmit power levels for all the BSs are lower as compared to those for $\eta = 0$. A reduction in the transmit power level of a BS reduces the signal power received by the MTs served by it. However, because the transmit power levels of the other BSs also reduce, the interference term in (2) also reduces. Thus, the reduction in power levels does not necessarily decrease the SINR (and thus the rate offered by the BSs and in turn the network latency) at the MTs. Rather, slightly better latency performance is realized due to better interference management when BSs are operating at lower transmit power levels. However, for large values of η (say $\eta = 10$), as can be seen from Figure 8, to save grid energy, the transmit power levels of the BSs are very low and additionally some of the BSs are switched off even during the peak traffic hours of the day (e.g. hour 16 (4 p.m.) to hour 20 (8 p.m.)). This increases the traffic that is handled by the BSs which are switched on and degrades the network latency performance. Additionally, as the transmit powers of the BSs decreases to very low levels, the impact of the reduced interference power on improving the SINR become marginal, and in many cases, the SINR degrades due to lower signal power. These two factors contribute the degradation of network latency at higher η values. Therefore, for higher values of η (e.g. $\eta = 10$), when η is increased,

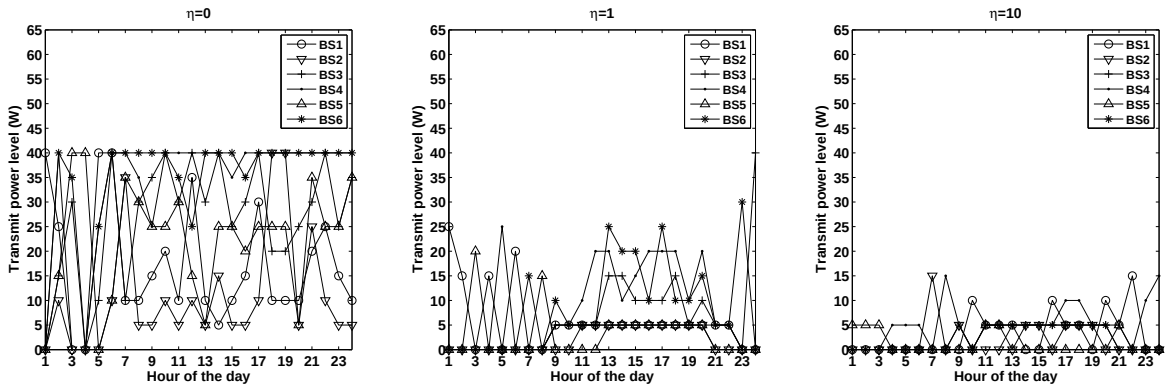

Fig. 8. Transmit power levels for the GD-RAM scheme for different η values (25^{th} January).

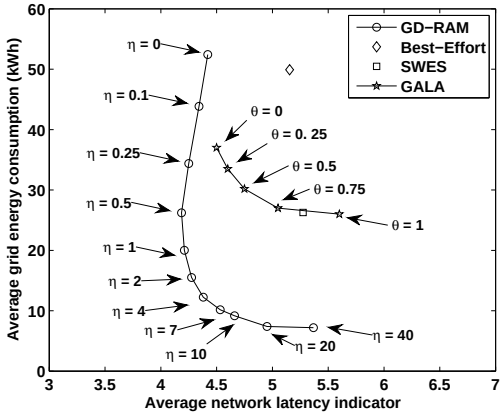

Fig. 9. Tradeoff between grid energy savings and average network latency.

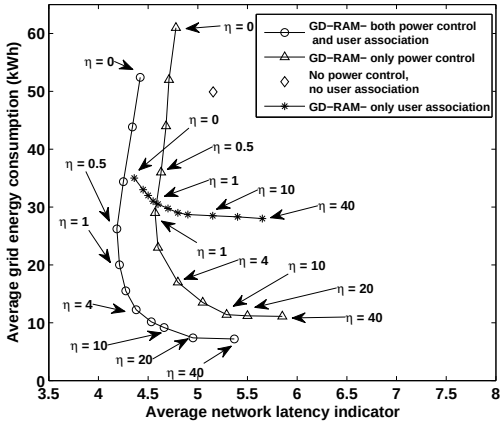

Fig. 11. Tradeoff between grid energy savings and average network latency for GD-RAM with and without power control and user-association.

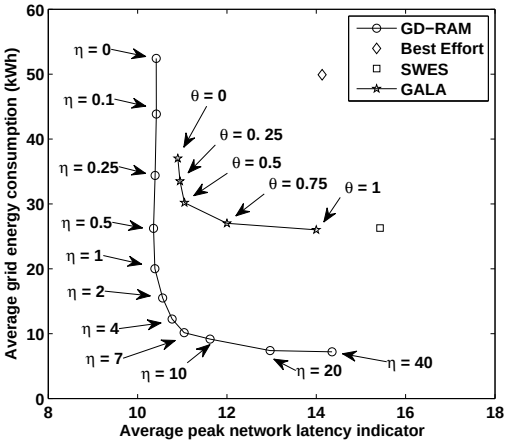

Fig. 10. Tradeoff between grid energy savings and peak network latency.

the energy savings are less significant whereas the increase in the delay for the marginal savings in the grid energy is very high. For a η value of 1 we observe that there is around 60% grid energy savings as compared to the traditional Best-Effort scheme while ensuring a better network latency performance. Additionally, in Figure 11 we present results showing the energy-delay trade-off for the GD-RAM scheme with and without power control and user-association. It is note-worthy that the power control operation is much more effective in reducing the energy consumption as compared to the use of user-association reconfiguration.

VII. Conclusion

In this paper we considered a network of grid connected solar powered BSs. We proposed a methodology for reducing the grid energy consumption while ensuring good quality of service. The methodology also gives the operator the freedom to mange the trade-off between the grid energy savings and the quality of service. The objective of reducing the grid energy consumption while maintaining the QoS was achieved by intelligent temporal energy allocation, BS downlink transmit power control and user association. A real BS deployment scenario and real solar energy traces were used to test the performance of the proposed methodology and to show its superiority over existing benchmark schemes. Compared to existing schemes, the proposed GD-RAM scheme provides control over trading energy for delay, and for a good choice of the trade-off factor (η), it can outperform all other benchmark

schemes in terms of minimizing the grid energy required while maintaining good quality of service.

REFERENCES

[1] V. Chamola and B. Sikdar, "Solar Powered Base Stations: Current Scenario, Issues and proposed Solutions," *IEEE Communications Magazine,* vol. 54, no. 5, pp. 108–114, May 2016.

[2] Global System Mobile Association (GSMA), accessed on Dec. 18, 2015. [Online]. Available: http://www.gsma.com/

[3] V. Chamola and B. Sikdar, "Resource Provisioning and Dimensioning for Solar Powered Cellular Base Stations", *Proc. IEEE GLOBECOM,* Austin, USA, 2014.

[4] M. A. Marsan, L. Chiaraviglio, D. Ciullo, and M. Meo, "Optimal energy savings in cellular access networks", *Proc. IEEE ICC*, Dresden, Germany, Jun. 2009.

[5] E. Oh, K. Son and B. Krishnamachari, "Dynamic base station switching-on/off strategies for green cellular networks," *IEEE Trans. Wireless Commun.,* vol 12, no. 5, pp. 2126-2136, 2013.

[6] J. Gong, J. S. Thompson, S. Zhou and Z. Niu, "Base station sleeping and resource allocation in renewable energy powered cellular networks," *IEEE Trans. Wireless Commun.,* vol. 62, no. 11, pp. 3801-3813, 2014.

[7] L.B. Le, D. Niyato, E. Hossain, D.I Kim and D.T Hoang,"QoS-aware and energy-efficient resource management in OFDMA femtocells," *IEEE Trans. Wireless Commun.,* vol. 12, no. 1, pp. 180-194, 2013.

[8] D. Ng, E. Lo and R. Schober, "Energy-efficient resource allocation in OFDMA systems with hybrid energy harvesting base station," *IEEE Trans. Wireless Commun.,* vol. 12, no. 7, pp. 3412-3427, 2013.

[9] T. Han and N. Ansari, "ICE: Intelligent Cell BrEathing to Optimize the Utilization of Green Energy," *IEEE Communications Letters,* vol. 16, no. 6, pp. 866-869, June 2012.

[10] Y. Mao, J. Zhang, and K. B. Letaief, " A lyapunov optimization approach for green cellular networks with hybrid energy supplies," *IEEE J. Sel. Areas Commun.*, vol. 33, no. 12, pp. 2463-2477, 2015.

[11] Q. Ye, B. Rong, Y. Chen, M. Al-Shalash, C. Caramanis and J. Andrews, "User association for load balancing in heterogeneous cellular networks," *IEEE Trans. Wireless Commun.*, vol. 12, no. 6, pp. 2706-2716, Jun. 2013.

[12] H. Kim, D. G. Veciana G, X. Yang and M. Venkatachalam, "Distributed-optimal user association and cell load balancing in wireless networks.," *IEEE/ACM Trans. Netw.*, pp. 177-90, Feb. 2012.

[13] T. Han and N. Ansari, "Green-energy aware and latency aware user associations in heterogeneous cellular networks," *Proc. IEEE GLOBECOM,* Atlanta, GA, USA, 2013.

[14] T. Han and N. Ansari, "A Traffic Load Balancing Framework for Software-Defined Radio Access Networks Powered by Hybrid Energy Sources," *IEEE/ACM Trans. Netw.,* vol. 24, no. 2, pp. 1038-1051, April 2016.

[15] D Liu, Y. Chen, K. K. Chai, and T. Zhang, "Distributed delay-energy aware user association in 3-tier HetNets with hybrid energy sources," *IEEE GLOBECOM Workshops,* Austin, TX, 2014.

[16] D. Liu, Y. Chen, K. Chai, T. Zhang, and M. Elkashlan, "Two-dimensional optimization on user association and green energy allocation for hetnets with hybrid energy sources," *IEEE Trans. Commun.,* vol. 63, no. 11, pp. 4111–4124, Nov. 2015.

[17] D. Liu et al., "User Association in 5G Networks: A Survey and an Outlook," *Commun. Surveys Tuts.,* vol. 18, no. 2, pp. 1018-1044, 2016.

[18] V. Chamola, B. Krishnamachari and B. Sikdar, "An Energy and Delay Aware Downlink Power Control Strategy for Solar Powered Base Stations", *IEEE Commun. Lett.* vol. 20, no. 5, pp. 954–957, May 2016.

[19] V. Chamola, B. Krishnamachari and B. Sikdar, "Green Energy and Delay Aware Downlink Power Control and User Association for off-Grid Solar Powered Base Stations," *IEEE Systems Journal*, Accepted for publication, pp. 1-12, Dec. 2016.

[20] L. Kleinrock, *Queueing Systems, vol. II: Computer applications*, Wiley-Interscience, New York, 1976.

[21] T. Han and N. Ansari, "Powering mobile networks with green energy," *IEEE Wireless Commun. Mag.*, vol. 21, no. 1, pp. 90-96, Feb. 2014.

[22] J. Fehske, F. Richter, and G. P. Fettweis , "Energy Efficiency Improvements through Micro Sites in Cellular Mobile Radio Networks," *Proc. IEEE GLOBECOM,* Honolulu, HI, Dec. 4, 2009.

[23] NREL Renewable Resource Data Center. Accessed Nov. 5, 2015. [Online]. Available: http://www.nrel.gov/rredc/solar_data.html

[24] T. Khatib , A. Mohamed and K. Sopian, "A review of solar energy modeling techniques," *Renewable and Sustainable Energy Reviews.*, vol. 16, iss. 5, pp. 2864-2869, 2012.

[25] G Reikard, "Predicting solar radiation at high resolutions: A comparison of time series forecasts," *Solar Energy* vol. 83, iss. 3, pp. 342-349, 2009.

[26] E. Oh and B. Krishnamachari, "Energy savings through dynamic base station switching in cellular wireless access networks," *Proc. IEEE GLOBECOM*, Miami, FL, Dec. 2010.

[27] M.Z. Shafiq, L. Ji, A.X. Liu and J. Wang, "Characterizing and modeling internet traffic dynamics of cellular devices," *Proc. ACM SIGMETRICS,* New York, NY, USA, 2011.

[28] X. Chen, Y. Jin, S. Qiang, W. Hu and K. Jiang, "Analyzing and modeling spatio-temporal dependence of cellular traffic at city scale," *Proc. IEEE ICC*, London, UK, 2015.

[29] U. Paul, A.P. Subramanian, M.M. Buddhikot and S.R. Das, "Understanding traffic dynamics in cellular data networks ," *Proc. INFOCOM*, Shanghai, China, 2011.

[30] D. Liu, Y. Chen, K.K. Chai, T. Zhang and K. Han, "Joint user association and green energy allocation in HetNets with hybrid energy sources," *Proc. WCNC*, LA, USA, 2015.

[31] T. Han and N. Ansari, "On optimizing green energy utilization for cellular networks with hybrid energy supplies," *IEEE Trans. Wireless Commun.*, vol. 12, iss. 8, pp. 3872-3882, 2013.

[32] K. Son, H. Kim, Y. Yi, and B. Krishnamachari, "Base station operation and user association mechanisms for energy-delay tradeoffs in green cellular networks," *IEEE J. Sel. Areas Commun.*, vol. 29, no. 8, pp. 1525-1536, Sep. 2011.

[33] S. Boyd and L. Vandenberghe, *Convex Optimization,* Cambridge University Press, 2004.

[34] Recommendation ITU-R M.1225, Guidelines for evaluation of radio transmission technologies for IMT-2000, 1997.

[35] IEEE 802.16m-08/004r5: IEEE 802.16m Evaluation Methodology Document (EMD), 2009

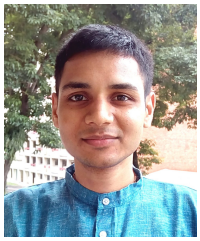

Vinay Chamola received his B.E. degree in electrical & electronics engineeerig and Master's degree in communication engineering from Birla Institute of Technology & Science (BITS), Pilani, India in 2010 and 2013 respectively. He received his Ph.D. degree in electrical and computer engineering from the National University of Singapore, Singapore, in 2016. From June to Aug. 2015, he was a visiting researcher at the Autonomous Networks Research Group (ANRG) at the University of Southern California (USC), USA. Currently he is a Research Fellow at the National University of Singapore. His research interests include solar powered cellular networks, energy efficiency in cellular networks, internet of things, and networking issues in cyberphysical systems.

Biplab Sikdar [S'98, M'02, SM'09] received the B.Tech. degree in electronics and communication engineering from North Eastern Hill University, Shillong, India, in 1996, the M.Tech. degree in electrical engineering from the Indian Institute of Technology, Kanpur, India, in 1998, and the Ph.D. degree in electrical engineering from the Rensselaer Polytechnic Institute, Troy, NY, USA, in 2001. He is currently an Associate Professor with the Department of Electrical and Computer Engineering, National University of Singapore, Singapore. His research interests include wireless MAC protocols, transport protocols, network security, and queuing theory.

Bhaskar Krishnamachari received his B.E. in Electrical Engineering at The Cooper Union, New York, in 1998, and his M.S. and Ph.D. degrees from Cornell University in 1999 and 2002 respectively. He is a Professor in the Department of Electrical Engineering at the University of Southern Californias Viterbi School of Engineering. His primary research interest is in the design and analysis of algorithms and protocols for next generation wireless networks.